

# Regulation of cholesterol and sphingomyelin metabolism by amyloid- $\beta$ and presenilin

Marcus O. W. Grimm<sup>1</sup>, Heike S. Grimm<sup>1</sup>, Andreas J. Pätzold<sup>1</sup>, Eva G. Zinser<sup>1</sup>, Riikka Halonen<sup>1</sup>, Marco Duering<sup>1</sup>, Jakob-A. Tschäpe<sup>1</sup>, Bart De Strooper<sup>2</sup>, Ulrike Müller<sup>3</sup>, Jie Shen<sup>4</sup> and Tobias Hartmann<sup>1\*</sup>

**Amyloid beta peptide (A $\beta$ ) has a key role in the pathological process of Alzheimer's disease (AD), but the physiological function of A $\beta$  and of the amyloid precursor protein (APP) is unknown<sup>1,2</sup>. Recently, it was shown that APP processing is sensitive to cholesterol and other lipids<sup>3-10</sup>. Hydroxymethylglutaryl-CoA reductase (HMGR) and sphingomyelinases (SMases) are the main enzymes that regulate cholesterol biosynthesis and sphingomyelin (SM) levels, respectively. We show that control of cholesterol and SM metabolism involves APP processing. A $\beta$ 42 directly activates neutral SMase and downregulates SM levels, whereas A $\beta$ 40 reduces cholesterol *de novo* synthesis by inhibition of HMGR activity. This process strictly depends on  $\gamma$ -secretase activity. In line with altered A $\beta$ 40/42 generation, pathological presenilin mutations result in increased cholesterol and decreased SM levels. Our results demonstrate a biological function for APP processing and also a functional basis for the link that has been observed between lipids and Alzheimer's disease (AD).**

One of the main characteristics of Alzheimer's disease (AD) is the accumulation of amyloid beta peptide (A $\beta$ ), which is associated with neurodegeneration<sup>1,2</sup>.

A $\beta$  production is initiated by the  $\beta$ -secretase cleavage of amyloid precursor protein (APP), which results in production of the APP C-terminal fragment C99. This fragment is further cleaved by  $\gamma$ -secretase to generate A $\beta$ 40 and A $\beta$ 42. The active centre of the  $\gamma$ -secretase complex is formed by presenilin-1 or -2 (PS1 or PS2)<sup>11</sup>. As the  $\gamma$ -secretase cleavage site is centred within the transmembrane domain, membrane composition may considerably influence A $\beta$  generation<sup>12</sup>. Such proteolytic events of regulated intra-membrane proteolysis (RIP) are involved in numerous cellular regulatory events, including lipid homeostasis<sup>13</sup>.

So far, the physiological role of APP and its proteolytic fragments, including A $\beta$ , have mainly been conceived as being brain specific. However, the ubiquitous production of APP, A $\beta$  and PS indicates that their functions are also ubiquitous.

Recently, strong evidence has accumulated that links AD and A $\beta$  generation with lipid homeostasis<sup>5</sup>, and it has been suggested that cellular lipid metabolism controls APP processing<sup>5</sup>. Studies have shown that A $\beta$  production is sensitive to cholesterol levels and lipid trafficking. *In vitro* enhanced cholesterol levels lead to increased A $\beta$  production<sup>14</sup>. Furthermore, cholesterol depletion reduces  $\gamma$ -secretase activity and results in reduced A $\beta$  generation<sup>3,4,6-9</sup>. Controversially, one report found a correlation between mildly decreased cholesterol levels and increased A $\beta$  production in Chinese hamster ovary cells<sup>15</sup>. *In vivo*, A $\beta$  production and deposition are tightly associated with changes in cholesterol levels<sup>6,10</sup>.

Lipid levels vary in response to changes in diet, and physical or neuronal activity. Similarly, A $\beta$  levels change in response to several conditions, including cholesterol and other factors<sup>16,17</sup>. Brain cholesterol levels increase during the progression of AD<sup>18</sup> and hypercholesterolaemia is an early risk factor in the development of AD<sup>19</sup>. Consequently, cholesterol-lowering drugs are being considered as a potential treatment for AD<sup>16,20,21</sup>. Nevertheless, the cellular mechanisms that link lipids, A $\beta$  generation and AD are poorly understood.

To investigate the role of PS in lipid regulation, we used mouse embryonic fibroblast cells that were devoid of PS1 and PS2 (MEF *PS1/2*<sup>-/-</sup>)<sup>11</sup> and expression-level-matched, A $\beta$ -producing PS re-transfected MEF *PS1/2*<sup>-/-</sup> control cells (MEF *PS1r* and MEF *PS2r*, respectively) (see Supplementary Information, Fig. S1). The absence of PS resulted in increased cellular levels of cholesterol and sphingomyelin (SM), but not phosphatidylcholine (PC) or total lipid-associated phosphate (Fig. 1a). The catabolic sphingomyelinase (SMase) activities were downregulated, anabolic SM-synthase activity was upregulated and the SM-to-ceramide ratio was increased in PS-deficient cells in accordance with the altered neutral SMase (nSMase) and SM-synthase activities (Fig. 1a, see Supplementary Information, Fig. S2a).

Absence of PS1 is lethal and, as PS2 is able to replace PS1 (for example, in nSMase activity, see Fig. 1c), brains from conditional PS1 knockout mice, crossed to PS2 knockout mice, were used to evaluate PS function in lipid homeostasis *in vivo*. In these viable mice, PS1 remains expressed

<sup>1</sup>Centre for Molecular Biology Heidelberg, INF 282, D-69120 Heidelberg, Germany. <sup>2</sup>Department of Human Genetics, VIB4 and KU Leuven, B-3000 Leuven, Belgium.

<sup>3</sup>Institute for Pharmacy and Molecular Biotechnology, INF 364, D-69120 Heidelberg, Germany. <sup>4</sup>Center for Neurologic Diseases, Brigham and Women's Hospital, Harvard Medical School, Boston, MA 02115, USA.

\*Correspondence should be addressed to T.H. (e-mail: Tobias.Hartmann@zmbh.uni-heidelberg.de)

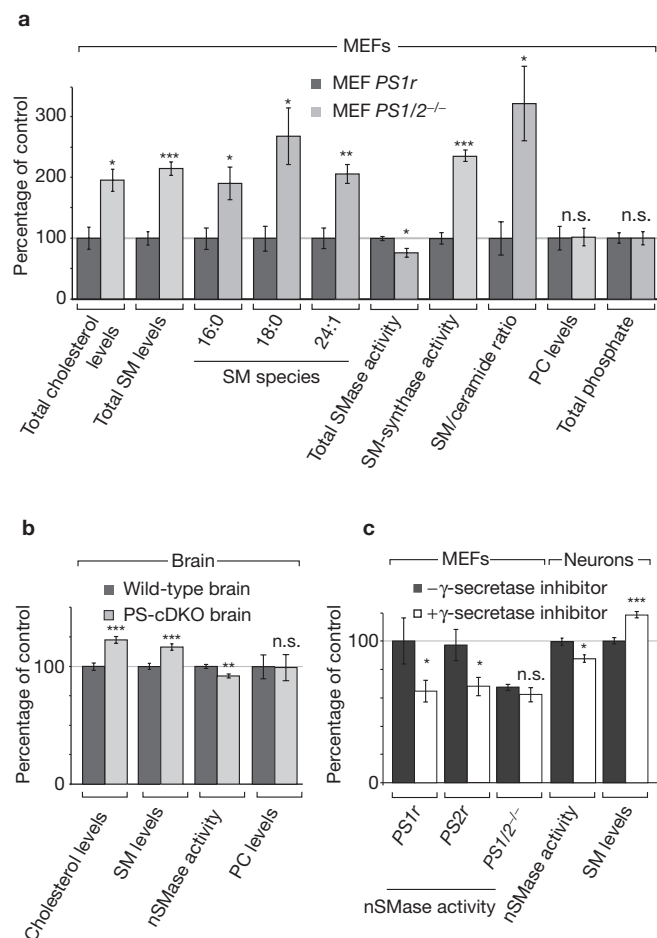


**Figure 1** Presenilin in lipid homeostasis. **(a)** Lipid and enzyme activity levels in presenilin 1/2 (*PS1/2*<sup>-/-</sup>) and *PS1* expression-rescued (*PS1r*) mouse embryonic fibroblasts (MEFs). Total sphingomyelin (SM) levels were determined by enzymatic assay; SM species and ceramide were determined by mass-spectrometry. Phosphatidylcholine (PC) levels represent the mean of major lipid species, as measured by mass-spectrometry. **(b)** Lipid and enzyme activity levels of cortical brain samples from PS-deficient mice (PS-cDKO) and wild type. The apparent decreased phenotype magnitude probably results from cells still possessing  $\gamma$ -secretase activity, due to pyramidal neuron-specific expression of Cre recombinase. **(c)** Effect of  $\gamma$ -secretase activity inhibition on nSMase activity in MEFs (all normalized to *PS1r*);  $\gamma$ -secretase activity is dependent on SMase activity and SM levels in primary mixed cortical wild-type mouse neurons (E14). \*  $P < 0.05$ ; \*\*  $P < 0.01$ ; \*\*\*  $P < 0.001$ ; and n.s. indicates that the results are not significant.

in some neurons and other cells<sup>22</sup> and brain A $\beta$  levels in these mice are reduced to 20–50%, depending on age and A $\beta$  species<sup>23</sup>. As before, absence of PS in neurons resulted in increased cholesterol and SM levels, decreased SMase activity, but unchanged PC levels (Fig. 1b).

Dependence on  $\gamma$ -secretase proteolytic activity was investigated using the  $\gamma$ -secretase activity inhibitor L-685,458. This treatment reduced nSMase activity in MEF *PS1r* and *PS2r* cells to similar levels as those of *PS1/2*<sup>-/-</sup> cells (Fig. 1c). By contrast, this inhibitor treatment had no effect on MEF cells that were devoid of PS (Fig. 1c). Treatment of wild-type mouse neurons decreased nSMase activity and increased SM levels (Fig. 1c). Accordingly, in inhibitor-treated PS-expressing cells, SM levels were increased. Cholesterol levels increased in MEF *PS1/2*<sup>-/-</sup> cells (Fig. 1a), whereas no significant difference was observed between inhibitor-treated MEF *PS1r* and MEF *PS1/2*<sup>-/-</sup> cells (see Supplementary Information, Fig. S2b).

It was established previously that cholesterol influences A $\beta$  production. To investigate a putative influence of SM on A $\beta$  production, we inhibited nSMase activity in neurons. This resulted in increased SM levels and decreased intracellular and secreted A $\beta$  (Fig. 2a). This was confirmed in COS7 cells using additional inhibitors and direct SM exposure (see Supplementary Information, Fig. S3a, 3b). Reduced  $\gamma$ -secretase cleavage causes C99 accumulation, which was observed with increased SM levels (see Supplementary Information, Fig. S3c).

Our results implicate the involvement of a  $\gamma$ -secretase substrate and that its cleavage is essential in PS-mediated lipid regulation. MEF *APP/APLP2*<sup>-/-</sup> and MEF wild-type cells were analysed to evaluate whether APP or APLP2 might be involved in this regulatory cascade. SM, nSMase activity and cholesterol levels responded to the absence of APP/APLP2 in the same way as they did to the absence of PS/ $\gamma$ -secretase activity (Fig. 2b). The same was observed in *APP*<sup>-/-</sup> mouse brain (Fig. 2b), suggesting that an *in vivo* function of APP exists in lipid homeostasis.

Unlike in wild-type cells, inhibition of  $\gamma$ -secretase activity did not alter cholesterol in MEF *APP/APLP2*<sup>-/-</sup> cells (Fig. 2c). This seems to rule out the existence of other  $\gamma$ -secretase substrates that are able to replace the APP/APLP2 function in cholesterol regulation in these cells. The combined necessity of APP and  $\gamma$ -secretase activity in this process indicates that a proteolytic APP fragment is involved in lipid homeostasis (Fig. 2b, c). The most prominent peptide that is derived from APP  $\gamma$ -secretase cleavage is A $\beta$ . To determine a possible function of A $\beta$  in cholesterol and SM regulation, we analysed key enzymes and metabolites in the respective pathways.

Analysing SM metabolism in MEF *APP/APLP2*<sup>-/-</sup> cells showed a decrease in nSMase activity compared with MEF wild-type cells (Fig. 2b). When exposed to A $\beta$ -containing conditioned media from human SH-SY5Y cells, the nSMase enzymatic activity was partially restored in MEF *APP/APLP2*<sup>-/-</sup> cells (Fig. 2d, left). To investigate whether this might be caused by A $\beta$ , cell homogenates of MEF *APP/APLP2*<sup>-/-</sup> cells were exposed to synthetic A $\beta$ 1–40/A $\beta$ 1–42 at a physiological ratio<sup>24</sup>, resulting in enhanced nSMase activity (Fig. 2d, right). To determine whether SMase is a molecular target for regulation by A $\beta$  and to evaluate whether this interaction might be direct, purified human placenta nSMase was exposed to synthetic A $\beta$  in a biochemical assay that was free of other cellular components. Covering the physiological concentration range of A $\beta$ <sup>24</sup>, the effect reached a maximum at peptide levels that are typically found in cerebrospinal fluid. The effect decreased thereafter, probably due to augmented peptide aggregation (Fig. 2e). An effect of A $\beta$  on the other assay components was excluded (see Supplementary Information, Fig. S4a); A $\beta$ 42–1 (inverse A $\beta$ ) was inactive and aggregated A $\beta$  had only residual stimulatory activity, presumably due to remnant non-aggregated peptide. An excess of A $\beta$ 40 reduced nSMase activation by A $\beta$ 42, indicating A $\beta$ 42 specificity (see Supplementary Information, Fig. S4b).

To evaluate the involvement of oxidative stress in nSMase activation by A $\beta$  peptides, the production of reactive oxygen species (ROS) was investigated. No significant differences in ROS were observed when wild-type and rescue cells were compared with the respective knockout cells (Fig. 2f). Incubation of MEF *PS1/2*<sup>-/-</sup> with A $\beta$  in the concentration range used above did not result in a concentration-dependent increase of ROS (Fig. 2e).

To investigate the regulation of cholesterol metabolism, MEF *APP/APLP2*<sup>-/-</sup> cells were treated with A $\beta$ , which reversed the effects that had been induced by the absence of APP/APLP2 (see Supplementary

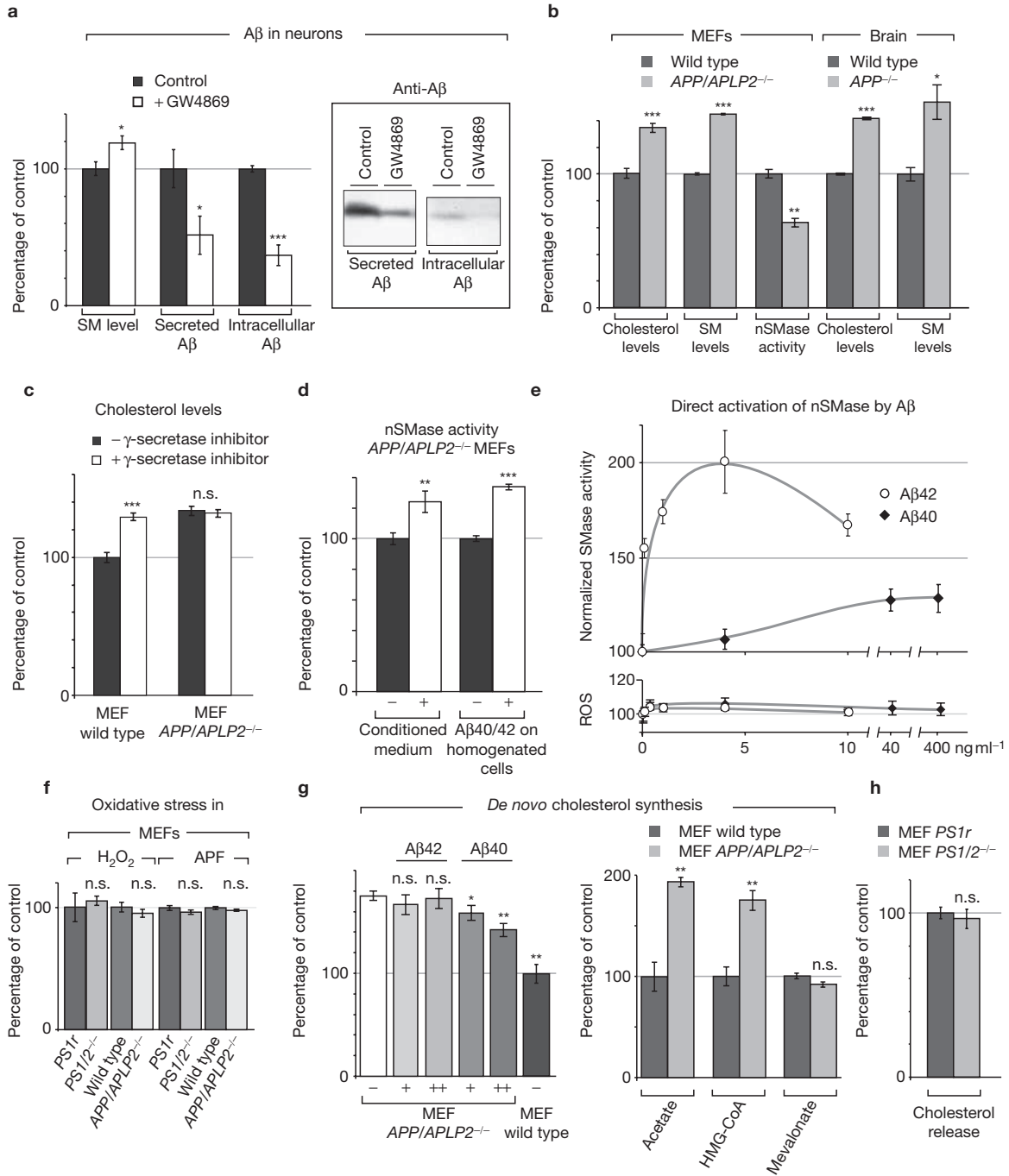


**Figure 2** Aβ and APP function in lipid homeostasis. (a) Decreased secreted and intracellular amyloid beta peptide (Aβ) generation following reduced sphingomyelin (SM) catabolism (GW4869, neutral sphingomyelinase (nSMase) activity inhibitor) in neurons. Inset: representative western blots. (b) Comparison of cholesterol, SM and nSMase activity in mouse embryonic fibroblasts (MEFs) in the presence or absence of APP/APLP2; lipid levels of total brain samples from APP-deficient mice (APP<sup>-/-</sup> brain) compared with the wild type. (c) MEF wild-type and MEF APP/APLP2<sup>-/-</sup> cells treated with L-685,458 γ-secretase activity inhibitor. Inhibition of γ-secretase activity increases cholesterol levels in MEF wild-type cells, whereas the absence of APP/APLP2 obliterates γ-secretase activity in cellular cholesterol homeostasis, as cholesterol levels remain unchanged following inhibition of γ-secretase activity. (d) Aβ increases nSMase activity. (left) MEF APP/APLP2<sup>-/-</sup> cells were incubated with medium containing Aβ secreted by SY5Y cells expressing SPC99. (right) Control for Aβ specificity: MEF APP/APLP2<sup>-/-</sup> cell homogenates incubated with synthetic Aβ (400 pg

Aβ40 + 40 pg Aβ42 [per ml]) show increased nSMase activity compared with untreated control. (e) Dose–response curve of purified human placenta nSMase activity to synthetic Aβ40 or Aβ42. ROS levels were determined in MEF PS1<sup>-/-</sup> cells by 3′-(p)-aminophenyl fluorescein (APF). (f) Comparison of oxidative stress in MEF PS1<sup>r</sup> versus MEF PS1<sup>2-/-</sup>, and MEF APP/APLP2<sup>-/-</sup> versus MEF wild-type cells, determined by H<sub>2</sub>O<sub>2</sub> and APF. (g) (left) Downregulation of cholesterol *de novo* synthesis after exposure of MEF APP/APLP2<sup>-/-</sup> to Aβ42 (0.04 (+) and 4 ng ml<sup>-1</sup> (++) or Aβ40 (0.4 (+) and 40 ng ml<sup>-1</sup> (++) in comparison with untreated APP/APLP2<sup>-/-</sup> and untreated wild-type cells. (right) Identification of hydroxymethylglutaryl-CoA reductase (HMGR) as the Aβ target in cholesterol *de novo* synthesis. MEF cells were incubated with the physiological precursors of cholesterol biosynthesis <sup>14</sup>C-acetate, the HMGR substrate <sup>14</sup>C-HMG-CoA or the HMGR product <sup>14</sup>C-mevalonate. (h) Cholesterol release was quantified following acetate incubation. \*P<0.05; \*\*P<0.01; \*\*\*P<0.001; and n.s. indicates that the results are not significant.

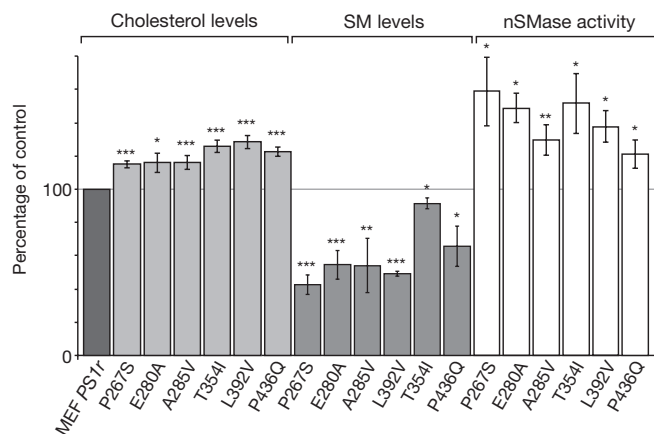


**Figure 3** Effects of PS-FAD mutations on cellular cholesterol, SM 18:0 levels and nSMase activity. Pathological PS-FAD mutations compared with *PS1r* in a MEF *PS1/2<sup>-/-</sup>* background. \*  $P \leq 0.05$ ; \*\*  $P \leq 0.01$ ; and \*\*\*  $P \leq 0.001$ .

Information, Fig. S4c). To ascertain the mechanism of A $\beta$  in cholesterol homeostasis, MEF *APP/APLP2<sup>-/-</sup>* cells were treated with the two A $\beta$  species separately and *de novo* synthesized cholesterol was analysed. In contrast to nSMase activity with A $\beta$ 40, which showed only a minor effect, *de novo* cholesterol synthesis responded already to low levels of A $\beta$ 40 and partially restored wild-type levels (Fig. 2g, left).

To identify the enzyme in the cholesterol biosynthetic pathway targeted by A $\beta$ , MEF *APP/APLP2<sup>-/-</sup>* cells were incubated with the hydroxymethylglutaryl-CoA reductase (HMGR) substrate HMG-CoA, or with mevalonate, the HMGR product. Increased *de novo* cholesterol synthesis was observed upon incubation with HMG-CoA, but not with mevalonate (Fig. 2g, right). Genotype-specific alterations in cellular cholesterol release could be excluded (Fig. 2h). This identifies HMGR as a target in the regulation of cholesterol *de novo* synthesis by APP/A $\beta$ .

The different effects of A $\beta$ 40 (HMGR inhibition) and A $\beta$ 42 (SMase activation) allow for a specific prediction of their activities in a cell-biological context. A change in A $\beta$ 40/42 ratio should lead to altered lipid levels. Familial PS mutations (PS-FAD) strongly increase A $\beta$ 42 and mildly decrease A $\beta$ 40 levels, without a relevant impact on the total A $\beta$  levels. Expression of PS-FAD mutations resulted in increased cholesterol and decreased SM levels, which was further confirmed by increased nSMase activity (Fig. 3). As predicted by the previous experiments, changes in the A $\beta$ 40/42 ratio alter lipid homeostasis.

In summary, our *in vivo* and *in vitro* data are consistent with a model (Fig. 4) in which the cascade of  $\gamma$ -secretase, APP processing and A $\beta$  peptides downregulate cholesterol and sphingolipid levels, which, in turn, regulate A $\beta$  generation. The molecular targets for A $\beta$  in the cholesterol and SM metabolic pathways are HMGR and nSMase, respectively.

The role of A $\beta$  in lipid homeostasis implies that its precursor APP has a function in lipid homeostasis, which is supported by altered lipid homeostasis in *APP<sup>-/-</sup>* mice.

We assume that additional  $\gamma$ -secretase substrates and cleavage products contribute to lipid homeostasis. This is supported by partial reversal of the lipid phenotype in cells following addition of A $\beta$  (Fig. 2g). Multiple  $\gamma$ -secretase products exist. Our data identify the involvement of A $\beta$ , but do not rule out the involvement of other fragments. In the MEF *APP/APLP2<sup>-/-</sup>* cells, lipid homeostasis could not be altered by inhibition of  $\gamma$ -secretase proteolytic activity. This identifies that APP/APLP2 in the MEF model are essential substrates. In addition, it rules out that, in

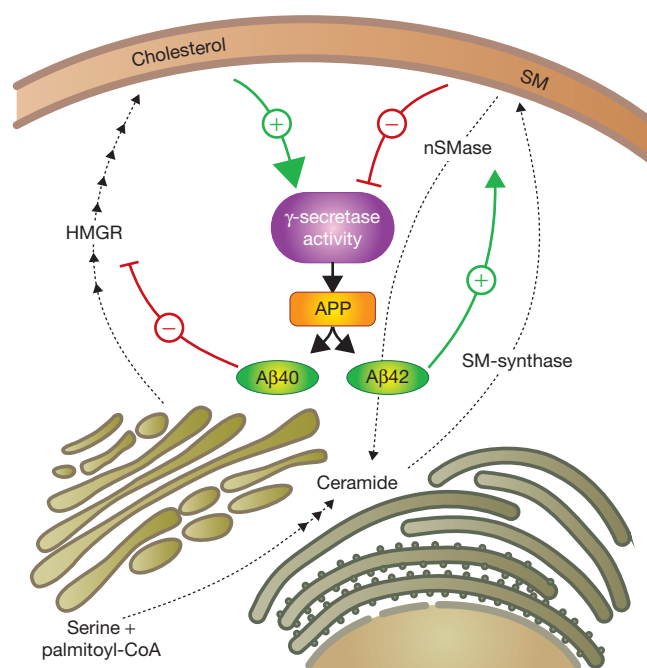


**Figure 4** Model of  $\gamma$ -secretase activity in lipid homeostasis. The  $\gamma$ -secretase activity regulates different lipid metabolic enzymes and lipid levels. This model predicts that the combined effects of cellular cholesterol and sphingomyelin (SM) levels control  $\gamma$ -secretase activity in amyloid precursor protein (APP) cleavage. This signal is then transmitted via amyloid beta peptide (A $\beta$ ) release to regulate lipid biosynthetic pathways, which differs for A $\beta$ 40 and A $\beta$ 42. SM levels are predominantly downregulated by A $\beta$ 42, due to activation of the SM degrading enzyme neutral sphingomyelinase (nSMase). By contrast, A $\beta$ 40 downregulates cholesterol *de novo* synthesis, due to inhibition of hydroxymethylglutaryl-CoA reductase (HMGR) activity. The interaction between A $\beta$ 42 and nSMase seems to be direct; it is currently unknown whether this is the case for the interaction of A $\beta$ 40 with HMGR. This regulation induces a feedback mechanism, as the same lipids that influence the  $\gamma$ -secretase microenvironment adjust the rate of  $\gamma$ -secretase cleavage of APP/C99 presumably by the concomitant change in membrane composition. The anticipated additional modulation by other  $\gamma$ -secretase substrates or products, further APP secretases and non- $\gamma$ -secretase lipid regulation are not implemented in this model.

the absence of APP/APLP2, other putative  $\gamma$ -secretase substrates have a detectable effect on SM and cholesterol homeostasis.

The  $\gamma$ -secretase-dependent regulation of lipid homeostasis is likely to be influenced by additional factors, as indicated by the other proteases that are involved in APP RIP and  $\gamma$ -secretase-independent regulatory cycles<sup>13</sup>.

In agreement with the ubiquitous presence of APP, A $\beta$  and PS<sup>25,26</sup>, the mechanism described here was found in cells of different origin.

Stimulation of SMase by addition of synthetic A $\beta$  peptides in the absence of any other modulating factors in a cell-free assay indicates that A $\beta$ 42 directly interacts with nSMase. This is consistent with the presence of an nSMase luminal/extracellular domain and the subcellular localizations of nSMases and A $\beta$ . Physiological A $\beta$ 42 concentrations were not previously investigated in this context, but high concentrations of A $\beta$ 42 or fibrillary A $\beta$ 42 were reported to cause oxidative stress, to affect lipid levels, but not cellular cholesterol content, and to stimulate nSMase *in vitro* by oxidative stress<sup>27,28</sup>. This may provide an alternative explanation for the direct interaction of A $\beta$  with SMase. ROS effects were previously observed to start occurring at A $\beta$  concentrations, coinciding with the highest A $\beta$ 42 levels used here. However, at this peptide concentration, nSMase activity already declined in our system. We observed, at the

comparatively low A $\beta$  concentrations used here, only marginal differences in ROS levels. This indicates that either low A $\beta$  levels produce ROS levels below our detection limit or that, in agreement with previous work<sup>28</sup>, low A $\beta$  concentrations do not trigger sufficient ROS production to explain the pronounced increase in SMase activity observed here. Reduced nSMase activity in the presence of additional A $\beta$ 40 (see Supplementary Information, Fig. S4b) and in the absence of a dose-dependent response of ROS to A $\beta$  indicates that a ROS-independent interaction is more likely. This may represent a remarkable difference between the physiological and pathological function of A $\beta$  at different peptide concentrations.

Properties of synthetic peptides may not reflect the *in vivo* situation. The cellular experiments with PS-FAD mutations were carried out on an endogenous APP background, without synthetic peptides or protein over-expression. As these experiments confirmed the conclusions drawn from the use of synthetic peptides, we have to assume that the experiments with synthetic peptides gave sufficiently valid mechanistic information.

Cholesterol,  $\gamma$ -secretase and A $\beta$  represent factors in a regulatory cycle: Cholesterol enhances  $\gamma$ -secretase activity, thereby yielding more A $\beta$ . A $\beta$ 40 suppresses HMGR activity, leading to decreased cholesterol levels. The absence of APP/APLP2 influences cholesterol *de novo* synthesis at the level of HMGR but not downstream of it, clearly identifying HMGR as the target. In principle, the structure of HMGR would allow a direct interaction with A $\beta$ , but it is currently unknown whether or not this actually occurs.

After the discovery of the lipid-controlled RIP mechanism of the sterol regulatory element binding protein (SREBP) with site-1 protease and site-2 protease (S2P), our findings characterize a second proteolytic system in lipid homeostasis. Although there are no sequence homologies, the functional analogies to the system presented here are striking<sup>13</sup>. Both systems act via HMGR, but an important difference is that APP processing reduces, whereas SREBP processing upregulates, cholesterol *de novo* synthesis. In a further analogy, the example of S2P suggests that not all  $\gamma$ -secretase substrates are processed lipid-dependently<sup>29</sup>.

The effect of PS-FAD mutations in SM homeostasis is inversed compared with cholesterol homeostasis, validating the stronger activation of nSMase by A $\beta$ 42 and the downregulation of *de novo* cholesterol synthesis by A $\beta$ 40. Notably, this differential regulation rules out SM homeostasis as a causative mediator of PS-dependent cholesterol levels.

Active involvement of APP cleavage, A $\beta$ ,  $\gamma$ -secretase activity and the effect of pathological PS-FAD mutations in lipid homeostasis provides a functional context for APP processing that has direct relevance for AD and may provide a rational basis for therapy.

## METHODS

**Cell culture.** COS7, human SH-SY5Y and MEF cells were cultivated in DMEM/10% fetal calf serum (FCS; not heat-inactivated); primary mixed cortical neurons from E14 mice (line C57B16) were cultivated to a density of 10<sup>6</sup> cells in N2-MEM for 7 d prior to experiments. Lipid exposure of COS7 cells was carried out in DMEM, with 0.1% delipidated FCS. Cell lines were transfected with pCEP4-SPC99 plasmid or pCDNA3.1-PS1 or pCDNA3.1-PS2. A $\beta$ -producing neurons were infected with SPC99 Semliki forest virus 6 h prior to collection of media or cell lysates<sup>6</sup>. Treatment with GW4869 (1  $\mu$ M) (Calbiochem, Darmstadt, Germany), 3-O-methylsphingomyelin (50  $\mu$ M) (Biomol, Hamburg, Germany), oxidised glutathione (5 mM) (Sigma, Taufkirchen, Germany), L-685,458 (1  $\mu$ M) (Calbiochem) or lovastatin (5  $\mu$ M) (Sigma) was performed for 24 h followed by 6 h conditioning in the presence of an inhibitor in DMEM/5% FCS for MEFs and COS7 cells, and in N2-MEM for neurons. SM (Biomol) was incubated for 24 h

with interjacent medium exchange, followed by 6 h conditioning in the presence of SM. It is important that cells are in the identical growth phase at the point that they reach confluency and are passage-matched (passages 3–8) to minimize variability in the cell-culture conditions. Treatment with synthetic A $\beta$  or A $\beta$  produced by SH-SY5Y-SPC99 cells (4 ml DMEM/10% FCS conditioned for 12 h) was performed in DMEM/10% FCS for 30 h with interjacent medium exchange at 6 h and 12 h. For experiments performed in the absence of FCS, cells were adapted by gradual FCS reduction.

**Sample preparation.** After washing confluent grown cells three times with 5 ml ice-cold phosphate-buffered saline (PBS), cells were scraped off in 500  $\mu$ l PBS. Cell or brain samples were homogenized using a Potter S at maximum speed for 1 min (B. Braun, Melsungen, Germany). Cortical brain samples were derived from cDKO PS1/2 mice that were sacrificed at 2 months of age and APP<sup>-/-</sup> mouse total brain samples were obtained 19.5 d *post-coitum*.

**Enzymatic assays.** Activity of SMase was measured using the Amplex-Red Sphingomyelinase Assay Kit (Molecular Probes, Karlsruhe, Germany). To analyse SMase activity in MEF cells and neurons, 0.2 mg protein was used; to analyse SMase and nSMase activity in mice brain, 0.4 mg protein was used.

Total SM concentrations were determined enzymatically using a modified assay from the Amplex-Red Sphingomyelinase Assay Kit (Molecular Probes). Briefly, for SM determination, samples were homogenized in PBS (pH 7.4) and adjusted to a protein concentration of 0.15 mg ml<sup>-1</sup> using a bicinchoninic acid assay. A 100  $\mu$ l sample was added to a 100  $\mu$ l assay solution, which contains 100  $\mu$ M Amplex Red reagent, 2 U ml<sup>-1</sup> HRP, 0.2 U ml<sup>-1</sup> choline oxidase, 8 U ml<sup>-1</sup> of alkaline phosphatase, 1 mU nSMase and 0.1 M Tris-HCl, 10 mM MgCl<sub>2</sub>, pH 7.4. After preincubation for 1 h at 37 °C under light exclusion conditions, fluorescence was measured for 30 min using excitation at 530  $\pm$  2.5 nm and fluorescence detection at 590  $\pm$  2.5 nm. The slope, which has to be 0, was calculated to scrutinize the completeness of the reaction. The values were corrected from the background signal that was determined by samples treated in the same way as described above but which did not contain any SMs.

Analysis of SM-synthase activity was performed, with modifications, according to Huitema *et al.*<sup>30</sup>. Cells were washed three times with RB2, pH 7.1 (120 mM K-glutamate, 20 mM HEPES-KOH, 5 mM NaCl, 2 mM MgCl<sub>2</sub>, 2 mM MnCl<sub>2</sub>, 15 mM KCl). Samples of 1 ml were diluted with RB2 to 2.5 mg ml<sup>-1</sup> and addition of 5  $\mu$ M nSMase inhibitor GW4869. The reaction was started by adding 2.5  $\mu$ l N-[acetyl-1-<sup>14</sup>C]-D-erythro-sphingosine (55 mCi/mmol; American Radiolabelled Chemicals, St Louis, MO). Lipids were extracted from the lipid phase after 2 h and lyophilized samples were resolved in 100  $\mu$ l CHCl<sub>3</sub>/methanol (1:2) and analysed using thin-layer chromatography.

**Assay for determining the direct stimulation of nSMase by A $\beta$ .** Only purified or synthetic components were used; cell extracts or other undefined components were not used. The effect of A $\beta$  on purified nSMase was determined in the presence of Mg<sup>2+</sup> by using 0.5 mU ml<sup>-1</sup> purified human placenta nSMase (Sigma), 0.5 mM SM (Molecular Probes), 8 U ml<sup>-1</sup> alkaline phosphatase, 0.2 U ml<sup>-1</sup> choline oxidase and 2 U ml<sup>-1</sup> horseradish-peroxidase (all obtained from Molecular Probes). Enzymatic activity was determined using Amplex-Red and calculation of the slope was carried out at 45 min-interval measurements. To exclude the effects of A $\beta$  on assay components other than nSMase, the identical components were used but nSMase was replaced by 0.1 mg ml<sup>-1</sup> cholinephosphate (Sigma).

**Cholesterol determination.** Cholesterol levels were determined using the Amplex-Red cholesterol assay (Molecular Probes). The same amount of protein as for the nSMase assay was used.

For cholesterol *de novo* synthesis, cells were incubated for 6 h with 0.2  $\mu$ Ci 3-hydroxy-3-methyl[3-<sup>14</sup>C]glutaryl-coenzyme-A, <sup>14</sup>C-mevalonate (1  $\mu$ Ci) or <sup>14</sup>C-acetate (1  $\mu$ Ci) (Amersham, Amersham, UK). Lipids were extracted and evaporated as described, resolved in 200  $\mu$ l CHCl<sub>3</sub>/methanol/HCl (5:10:0.075); 2.5 ml of scintillation solution Ultima Gold (Packard Instruments, Meriden, CT) was added and thoroughly vortexed for 30 min. Incorporation of the radioactive precursors into cholesterol was determined using a LS 6000IC scintillation counter (Beckman-Coulter, Krefeld, Germany). For cholesterol release, cells were treated with <sup>14</sup>C-acetate (1  $\mu$ Ci) for 6 h. Lipids of the medium were extracted and radioactive cholesterol was measured as described previously.

**Oxidative stress.** ROS was determined by 3'-(p)-aminophenyl fluorescein (APF) (Invitrogen, Karlsruhe, Germany). After homogenization of MEF cells, a protein concentration of 0.1 mg ml<sup>-1</sup> in PBS (pH 7.4) was incubated in the presence of 50 μM APF for 5 min before fluorescence was measured (excitation/emission: 490/515 nm).

Hydrogen peroxide was measured using Amplex-Red (Molecular Probes). To determine H<sub>2</sub>O<sub>2</sub> concentration in MEF cells, 0.15 mg protein was used. Amplex-Red was added to homogenized cells and incubated for 40 min at 37 °C in PBS (pH 7.4) before fluorescence was measured (excitation/emission: 530/590 nm).

**Aβ analysis and antibodies.** Aβ/C99 detection and quantification were determined as published previously<sup>6</sup>. W02 was directed against Aβ, G2-10 against Aβ40 and G2-11 against Aβ42.

**Peptides.** Aβ peptides were obtained from Bachem or Botond Penke (Szeged, Hungary). Aggregated Aβ42 (0.1 mg ml<sup>-1</sup>) was produced by incubation for 5 d at 37 °C.

**Statistical analysis.** All quantified data represent an average of at least three independent experiments. Error bars represent standard deviation of the mean. Statistical significance was determined by two-tailed Students t-test; significance was set at \*  $P \leq 0.05$ ; \*\*  $P \leq 0.01$ ; and \*\*\*  $P \leq 0.001$ . (See Supplementary Information for complete descriptions of Methods).

Note: Supplementary Information is available on the Nature Cell Biology website.

#### ACKNOWLEDGEMENTS

We are grateful to I. Tomic and R. Stammann for excellent technical assistance; B. Penke for peptides; T. Ruppert for mass-spectrometry advice and support; and for funding received from the European Union via QLK-172-2002 *Lipidiet*, Deutsche Forschungsgemeinschaft and Bundesministerium für Bildung und Forschung.

#### COMPETING FINANCIAL INTERESTS

The authors declare that they have no competing financial interests.

Published online at <http://www.nature.com/naturecellbiology/>

Reprints and permissions information is available online at <http://npg.nature.com/reprintsandpermissions/>

- Hardy, J. & Selkoe, D. J. The amyloid hypothesis of Alzheimer's disease: progress and problems on the road to therapeutics. *Science* **297**, 353–356 (2002).
- Sisodia, S. S. & St George-Hyslop, P. H.  $\gamma$ -Secretase, Notch, A $\beta$  and Alzheimer's disease: where do the presenilins fit in? *Nature Rev. Neurosci.* **3**, 281–290 (2002).
- Wahrle, S. *et al.* Cholesterol-dependent  $\gamma$ -secretase activity in buoyant cholesterol-rich membrane microdomains. *Neurobiol. Dis.* **9**, 11–23 (2002).
- Burns, M. *et al.* Presenilin redistribution associated with aberrant cholesterol transport enhances  $\beta$ -amyloid production *in vivo*. *J. Neurosci.* **23**, 5645–5649 (2003).
- Puglielli, L., Tanzi, R. E. & Kovacs, D. M. Alzheimer's disease: the cholesterol connection. *Nature Neurosci.* **6**, 345–351 (2003).
- Fassbender, K. *et al.* Simvastatin strongly reduces levels of Alzheimer's disease  $\beta$ -amyloid peptides A $\beta$ 42 and A $\beta$ 40 *in vitro* and *in vivo*. *Proc. Natl Acad. Sci. USA* **98**, 5856–5861 (2001).
- Runz, H. *et al.* Inhibition of intracellular cholesterol transport alters presenilin localization and amyloid precursor protein processing in neuronal cells. *J. Neurosci.* **22**, 1679–1689 (2002).
- Yamazaki, T., Chang, T. Y., Haass, C. & Ihara, Y. Accumulation and aggregation of amyloid  $\beta$ -protein in late endosomes of Niemann-pick type C cells. *J. Biol. Chem.* **276**, 4454–4460 (2001).
- Sawamura, N. *et al.* Modulation of amyloid precursor protein cleavage by cellular sphingolipids. *J. Biol. Chem.* **279**, 11984–11991 (2004).
- Refolo, L. M. *et al.* A cholesterol-lowering drug reduces  $\beta$ -amyloid pathology in a transgenic mouse model of Alzheimer's disease. *Neurobiol. Dis.* **8**, 890–899 (2001).
- Herreman, A. *et al.* Total inactivation of  $\gamma$ -secretase activity in presenilin-deficient embryonic stem cells. *Nature Cell Biol.* **2**, 461–462 (2000).
- Grziwa, B. *et al.* The transmembrane domain of the amyloid precursor protein in microsomal membranes is on both sides shorter than predicted. *J. Biol. Chem.* **278**, 6803–6808 (2003).
- Brown, M. S., Ye, J., Rawson, R. B. & Goldstein, J. L. Regulated intramembrane proteolysis: a control mechanism conserved from bacteria to humans. *Cell* **100**, 391–398 (2000).
- Simons, M. *et al.* Cholesterol depletion inhibits the generation of  $\beta$ -amyloid in hippocampal neurons. *Proc. Natl Acad. Sci. USA* **95**, 6460–6464 (1998).
- Abad-Rodriguez, J. *et al.* Neuronal membrane cholesterol loss enhances amyloid peptide generation. *J. Cell Biol.* **167**, 953–960 (2004).
- Simons, M. *et al.* Treatment with simvastatin in normocholesterolemic patients with Alzheimer's disease: a 26-week randomized, placebo-controlled, double-blind trial. *Ann. Neurol.* **52**, 346–350 (2002).
- Shoji, M. *et al.* The levels of cerebrospinal fluid A $\beta$ 40 and A $\beta$ 42(43) are regulated age-dependently. *Neurobiol. Aging* **22**, 209–215 (2001).
- Cutler, R. G. *et al.* Involvement of oxidative stress-induced abnormalities in ceramide and cholesterol metabolism in brain aging and Alzheimer's disease. *Proc. Natl Acad. Sci. USA* **101**, 2070–2075 (2004).
- Pappolla, M. A. *et al.* Mild hypercholesterolemia is an early risk factor for the development of Alzheimer amyloid pathology. *Neurology* **61**, 199–205 (2003).
- Wolozin, B., Kellman, W., Ruosseau, P., Celesia, G. G. & Siegel, G. Decreased prevalence of Alzheimer disease associated with 3-hydroxy-3-methylglutaryl coenzyme A reductase inhibitors. *Arch. Neurol.* **57**, 1439–1443 (2000).
- Sparks, D. L. *et al.* Atorvastatin for the treatment of mild to moderate Alzheimer disease: preliminary results. *Arch. Neurol.* **62**, 753–757 (2005).
- Saura, C. A. *et al.* Loss of presenilin function causes impairments of memory and synaptic plasticity followed by age-dependent neurodegeneration. *Neuron* **42**, 23–36 (2004).
- Beglopoulos, V. *et al.* Reduced  $\beta$ -amyloid production and increased inflammatory responses in presenilin conditional knock-out mice. *J. Biol. Chem.* **279**, 46907–46914 (2004).
- Ida, N. *et al.* Analysis of heterogeneous  $\beta$ A4 peptides in human cerebrospinal fluid and blood by a newly developed sensitive Western blot assay. *J. Biol. Chem.* **271**, 22908–22914 (1996).
- Lee, M. K. *et al.* Expression of presenilin 1 and 2 (PS1 and PS2) in human and murine tissues. *J. Neurosci.* **16**, 7513–7525 (1996).
- Slunt, H. H. *et al.* Expression of a ubiquitous, cross-reactive homologue of the mouse  $\beta$ -amyloid precursor protein (APP). *J. Biol. Chem.* **269**, 2637–2644 (1994).
- Jana, A. & Pahan, K. Fibrillar amyloid- $\beta$  peptides kill human primary neurons via NADPH oxidase-mediated activation of neutral sphingomyelinase: implications for Alzheimer's disease. *J. Biol. Chem.* **279**, 51451–51459 (2004).
- Qi, X. L. *et al.* Oxidative stress induced by  $\beta$ -amyloid peptide (1–42) is involved in the altered composition of cellular membrane lipids and the decreased expression of nicotinic receptors in human SH-SY5Y neuroblastoma cells. *Neurochem. Int.* **46**, 613–621 (2005).
- Haze, K., Yoshida, H., Yanagi, H., Yura, T. & Mori, K. Mammalian transcription factor ATF6 is synthesized as a transmembrane protein and activated by proteolysis in response to endoplasmic reticulum stress. *Mol. Biol. Cell* **10**, 3787–3799 (1999).
- Huitema, K., van den Dikkenberg, J., Brouwers, J. F. & Holthuis, J. C. Identification of a family of animal sphingomyelin synthases. *EMBO J.* **23**, 33–44 (2004).